LA-UR-83-2144

Conf-830719--17

LA-UR--83-2144

DE83 015916

Los Alamos National Laboratory is operated by the University of California for the United States Department of Energy under contract W-7405-ENG-36

TITLE RAREFACTION VELOCITIES IN SHOCKED TANTALUM AND THE HIGH-PRESSURE MELTING POINT

AUTHOR(S) J. M. Brown, VSM M-6
J. W. Shaner, M-6

SUBMITTED TO Proceedings of the American Physical Society 1983 Topical Conference on Shock Waves in Condensed Matter, 18-21 July 1983 Santa Fe, NM.

DISCLAIMER

Los Alamos Los Alamos National Laboratory
Los Alamos, New Mexico 87545

RAREFACTION VELOCITIES IN SHOCKED TANTALUM AND THE HIGH PRESSURE MELTING POINT

J. M. Brown
Texas A&M University
College Station, Texas

and

J. W. Shaner
Los Alamos National Laboratory
Los Alamos, New Mexico 87545

The optical analyzer technique has been used to determine the pressure at which a shock compressed tantalum can no longer support a longitudinal elastic wave. At 295 GPa, the release wave velocity drops to a value consistent with a calculated bulk sound velocity, indicating partial melting. At higher shock pressures, the bulk sound velocity follows a constant $\rho\gamma$ model, where γ is the Grüneisen parameter. With these measurements we have identified melting on the Ta Hugoniot, and we have calibrated Ta as a high impedance driver for similar experiments on other materials.

INTRODUCTION

A universal problem in the behavior of materials at high pressures is the location of the melting phase boundary. The scientific interest lies in being able to predict this phase change over wide density variations. However, in applications of shocked materials this phase boundary is also important for computational design. For example, we expect material strength and effective viscosity to change dramatically upon melting.

A thermodynamically correct approach to calculating the melting line consists of evaluating Gibbs free energies for the liquid and solid phases as a function of pressure and temperature, and identifying the locus of the intersection of these two surfaces. This basic approach has been applied to the simple nearly-free-electron metal Na with some success.(1) In general, however, the results of this calculation are severely model dependent, and sufficiently accurate thermodynamic parameters are often lacking. In the absence of an accurate theoretical model, various phenomenological and purely empirical relations are often used for extrapolation. For example, in Lindemann's phenomenological model, melting is assumed to occur at a critical ratio of mean thermal displacement of the atoms to the equilibrium nearest neighbor distance.(2) If this critical ratio is independent of compression, and if all vibration frequencies have the same volume dependence,

$$\frac{d\ln T_m}{d\ln V} = 2\gamma - \frac{2}{3} \qquad (1)$$

where T_m is the melting temperature, and γ is the vibrational Grüneisen parameter. Frequent criticisms of the Lindemann criterion are that the critical ratio cannot be calculated from first principles and that thermodynamic properties of only the solid are used.

Other purely empirical rules include the Simon equation, (3) which is merely a functional fit to the characteristic shape of melting curves, and the Kraut-Kennedy rule (4)

$$T_m = T_m^0(1 + C\frac{\delta V}{V}) \quad . \qquad (2)$$

This latter rule is the first order Taylor expansion for the melting temperature as a function of compression.

A significant problem with the phenomenological and empirical fits is that although agreement with experimental data can be forced for modest compressions (≤10%), the predictions diverge at higher compressions. For example, the spread of predicted melting temperatures for iron at 400 GPa is 400 K to 12000 K.(5)

The thermodynamic states behind strong shocks are particularly appropriate for melting studies. The positive curvature of temperature as a function of shock pressure means that the principal Hugoniot will always cross normal melting lines.(6) Also the inertial confinement allows measurements at densities and temperatures that are inaccessible to static techniques.

The question of whether equilibrium melting could be measured in the short time of a shock experiment was answered several years ago by Asay. (7,8) He noted, for materials that

melted at temperatures low enough for direct comparison of shock and static data, that when the Hugoniot crossed the solidus, the velocity of the head of the release wave dropped rapidly from the longitudinal to the bulk sound velocity. These velocities differ by ~30%. A detection technique, called the optical analyzer, which allows similar measurements at arbitrarily high pressures was recently reported.(9) We have used this technique previously to detect a solid-solid phase change and melting in iron at shock pressures above 200 GPa.(10) We report here similar data for tantalum between 210 and 440 GPa.

EXPERIMENTAL TECHNIQUE

We measure the velocities of rarefaction waves overtaking a shock wave in these experiments. Shock waves, generated by the impact of a high velocity thin flyer on a target, propagate into both the impactor and target. At the back surface of the impactor, the interaction of the shock wave with the interface between impactor and plastic sabot generates a rarefaction wave which propagates back through the impactor and target. The rarefaction overtakes the shock front and releases pressure. A transparent, high density material is placed over a target with steps of different thicknesses. Shock propagation into the analyzer material causes large shock heating, accompanied by thermal radiation in the visible spectrum. The overtaking of the shock by the rarefaction wave causes a reduction in pressure and temperature. Thus, a sharp decrease in thermal radiation results. The variation in target thicknesses leads to different time intervals between emergence of the shock in the analyzer and overtaking of the shock by the rarefaction. Since the thermal radiation intensity varies as a high power of the temperature, or pressure, this technique is especially sensitive to small pressure changes.

We detect visible light output from the optical analyzer above each target level. Apertures and baffles collimate the thermal radiation, which is transported through silica optical fibers to photomultiplier detectors. Single sweep, internally triggered oscilloscope records are obtained for four target levels on each experiment.

A discontinuous increase in signal amplitude occurs as the shock emerges from the tantalum into the analyzer. Nearly constant thermal radiation is observed as the shock moves through the analyzer. The rarefaction overtaking point is marked by declining radiation intensity. The time intervals, Δt, between shock emergence and overtaking point are determined with a reproducibility of approximately one nanosecond. These values are plotted against target thickness, and a short linear extrapolation defines the thickness at which the rarefaction would overtake the shock front at the target-analyzer interface. This extrapolation procedure allows us to experimentally eliminate problems associated with reflected waves from this interface.

The quantity R is defined to be the ratio of target thickness at the rarefaction overtaking point to impactor thickness. We further define

$$R^* = (1+R)/(1-R), \tag{3}$$

which is related to the rarefaction velocity, C, shock velocity U_s, and relative density ρ/ρ_o, by

$$R^* = \left(\frac{\rho}{\rho_o}\right)\frac{C}{U_S} \quad . \tag{4}$$

The thermodynamic quantity dE/dP_v can be determined from the finite difference equation (11)

$$\frac{dE}{dP_v} = \left[\frac{dE}{dV_H} - \frac{dE}{dV_S}\right]/\left[\frac{dP}{dV_H} - \frac{dP}{dV_S}\right] \tag{5}$$

where partial derivatives are along the Hugoniot (H) or isentrope (S). Using the Rankine-Hugoniot relations and a linear relation between shock velocity (U_s) and particle velocity (U_p), (12)

$$U_s = C_o + S\,U_p \quad , \tag{6}$$

equation (4) can be written as

$$\frac{dE}{dP_v} = \frac{Sn^2}{\rho_o}\left[(1+Sn) - R^*(1-Sn)\right]^{-1} \quad , \tag{7}$$

where n is $(V_o-V)/V$ which is equal to U_p/U_s.

RAREFACTION VELOCITIES FOR TANTALUM

We show results for eleven experiments in Fig. 1.

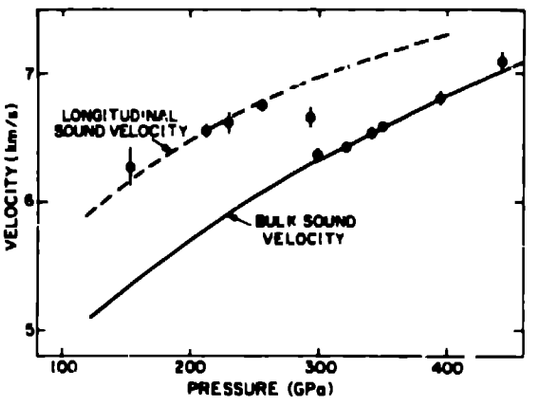

Figure 1: Rarefaction sound velocities as a function of Hugoniot pressure for tantalum. The solid curve is calculated for a constant value of dE/dP_V. The dashed line represents a linear pressure dependance of Poisson's ratio.

A marked discontinuity occurs near a pressure of 295 GPa. Data at higher pressure are well represented by a curve calculated for a bulk sound velocity with the parameter, dE/dP_V constant. Higher velocities, observed at lower pressure, are consistent with longitudinal elastic wave velocities. The curves shown in Fig. 2 were calculated from the Hugoniot data and $\rho\gamma$ = constant for the bulk sound velocity, and Poisson's ratio, $\nu = 0.35 + 24\times10^{-6}P$ (GPa) for the longitudinal sound velocity. All lower pressure records also show characteristic 'elastic-plastic' behavior (i.e. an extra kink when the plastic wave arrives) while at higher pressure the rarefaction pressure release is smooth.

DISCUSSION

Application of Eq. (1) to the melting of tantalum requires care in choice of a model for $\gamma(V)$. If all vibrational frequencies have the same volume dependence, and if temperatures are above the Debye temperature, so all vibrational modes are thermally populated, deviations between the thermodynamic Grüneisen parameter and the lattice vibration value must be associated with electronic contributions. Removal of an electronic contribution is a nontrivial problem. Our data is consistent with $\rho\gamma$ = constant, and $\gamma_0 = 1.80$ at STP. The value of γ_0 from thermodynamic parameters is 1.65. Boechmeiber gives a value of 1.82 for the thermodynamic γ with electronic contribution removed.(11) However, his procedure of removing the electronic contribution to C_V is not rigorously correct. Another approach to determining what γ value to use in Eq. (1) is to match the initial melting slope of 60±10K/GPa.(14) The bulk modulus at the normal melting point must also be known. By extrapolating Soga's data on the temperature dependence of elastic constants for tantalum (15) and using Eq. (1) we estimate γ_0 to be 1.7±0.3 at the normal melting point. A spread in melting predictions using the Lindemann criterion with $\rho\gamma$ = constant and an initial γ from 1.6 to 2.0 is shown in Fig. 2. This range represents our uncertainty in applying the Lindemann criterion to this refractory metal.

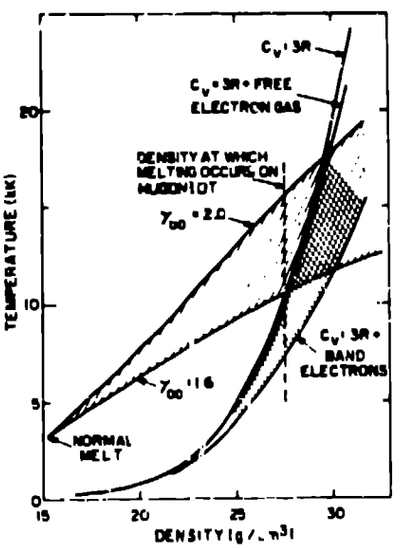

Figure 2: Lindemann melting curves and Hugoniot temperatures for tantalum. Curves based on differing assumptions for γ_0 and C_V are marked.

Electronic contributions are also problematic in calculation of temperatures along the shock Hugoniot for tantalum. Shock temperatures can be calculated from (11)

$$dT = -T\left(\frac{\gamma}{V}\right)dV + \frac{1}{2C_V}\left[(V_0-V)dP + (P-P_0)dV\right] \quad (8)$$

Although Eq. (8) also depends on γ, we find that the largest errors in Hugoniot temperatures are due to uncertain electronic contributions to heat capacity. The heat capacity is written

$$C_V = D + B_e T \quad (9)$$

where D is the Debye function and B_e is proportional to the electron mass at the Fermi surface. For a free electron gas, B_e is proportional to the reciprocal of the Fermi energy and therefore, to $V^{+2/3}$ where V is the specific volume. With this density depend-

ence, we inherently assume that the number of free electrons per ion remains unchanged. For five electrons per ion at normal density, β_e is equal to 0.25 mJ mole^{-1}K^{-3} for tantalum.

An empirical determination of β_e consists of measuring the component of C_v linear in T at low temperatures. Such measurements give β_e = 5.9 mJ mole^{-1}K^{-2}.(16) This large value is due to the location of the Fermi surface near a d-band peak in the electronic density of states, and clearly shows the unsuitability of the free electron gas model for transition metals.

An alternative analysis is based on the realization that the electron-phonon mass enhancement may be large, particularly for low mobility d-electrons at low temperatures. McMillan provided an expression relating the mass enhancement factor, g, to the superconducting transition temperature.(17) For tantalum the result is g = 0.69. Since β_e is proportional to electronic mass, it should be divided by 1.69 to get the value appropriate for unrenormalized electrons. This new value of 3.5 mJ mole^{-1}K^{-2} agrees well with rigid lattice APW calculations.(18) Since the electron-phonon mass enhancement turns off for temperatures above the Debye temperature (19), this value is the most realistic.

Three model Hugoniots are plotted in Fig. 2. The highest temperature estimates ignore the electronic contribution to heat capacity. Much lower temperatures result with band electron contributions to heat capacity included. The intermediate curve, calculated for a free electron gas contribution, may be appropriate at the highest temperatures. As temperatures increase, the density of electronic states within kT of the Fermi level must decrease. Furthermore, with high-pressure volume compression, the d-bands will broaden leading to lower densities of electronic states. Finally, high temperatures can cause thermal ionization. This increases the conduction electron density, which decreases β_e by $Z^{-2/3}$, where Z is the degree of ionization. With all these effects combined, calculation of Hugoniot temperatures remains a challenging problem.

The melting point observed in these experiments occurs at a lower Hugoniot pressure than any reasonable choice for the Lindemann law or Hugoniot temperatures. This situation was also noted for Iron, (10) but the disagreement is somewhat worse for tantalum. However, without a rigorous calculation of the free energies of the solid and liquid phases of the more complex metals, the Lindemann criterion appears to provide a close upper bound on the melting line.

ACKNOWLEDGEMENTS

This work was funded in part by the National Science Foundation (EAR 81-09591) and by the Department of Energy.

REFERENCES

1. Stroud, D. and Ashcroft, N. W., Phys. Rev. B 55 (1972) 371.

2. Lindemann, F.A., Phys. Z., 11 (1910) 609.

3. Babb,S.E., Rev. Mod. Phys. 35 (1963) 400.

4. Kraut, E. A. and Kennedy, G. C., Phys. Rev. 151 (1966) 668.

5. Boschi, E., in Physics of the Earth's Interior A. M. Dziewonski and E. Boschi (eds.), (North-Holland, Amsterdam 1980).

6. By normal melting we mean dT_m/dP is positive but decreases with pressure.

7. Asay, J.R., J. Appl. Phys. 48 (1977) 2837.

8. Asay, J. R. and Hayes, D. B., J. Appl. Phys. 46 (1975) 4789.

9. McQueen, R. G., Hopson, J. W., Fritz, J. N., Rev. Sci. Inst. 53 (1982) 245.

10. Brown, J. M. and McQueen, R. G., Geophys. Res Lett 7 (1980) 533.

11. McQueen, R. G. in Laboratory Techniques for Very High Pressures and the Behavior of Metals, edited by Gschneidner, K. A., M. T. Hepworth, and Parlee, N. A. D., Metall. Soc. Conf. 22 (1964).

12. Parameters for tantalum are given by: Mitchell, A. C. and Nellis, W. J., J. Appl. Phys. 52 (1981) 3363.

13. Gschneidner, K. A., Solid State Phys. 16 (1969).

14. Shaner, J.W., Gathers, G.R. and Minichino, C., High Temp-High Press. 9, (1977) 331.

15. Sogo, S., J. Appl. Phys., 37 (1963) 3416.

16. Kittel, C., Introduction to Solid State Physics, 4th Ed. p 254, (Wiley and Sons, New York, 1971).

17. McMillan, W.L., Phys. Rev. 167 (1968) 331.

18. Matheiss, L., Phys. Rev B 1 (1971) 171.

19. Grimvall, G., Phys. Scr., 14 (1976) 63.